Journal of Biomolecular NMR (2005) 31: 161–166 © Springer 2005

Suppression of anti-TROSY lines in a sensitivity enhanced gradient selection TROSY scheme

Daniel Nietlispach
Department of Biochemistry, University of Cambridge, 80 Tennis Court Road, Cambridge CB2 1 GA, U.K.

Received 16 November 2004; Accepted 17 December 2004

Key words: anti-TROSY, NOESY, sensitivity enhancement, spin-state selective, ST2-PT, TROSY

Abstract

A simple modification of the TROSY pulse transfer scheme, suggested by Yang and Kay [J. Biomol. NMR 13 (1999) 3–10], is proposed which results in the suppression of unwanted anti-TROSY lines without any extra loss in sensitivity. The higher sensitivity of this TROSY transfer scheme therefore becomes available for 2D [^{15}N, ^{1}H] TROSY correlation and 3D/4D ^{15}N separated NOESY type experiments where complete suppression of the broad anti-TROSY lines is essential.

Introduction

Two general types of $^{1}H_N/^{15}N$ TROSY implementations have been reported so far. The ST2-PT (single-transition to single-transition) based experiments (Pervushin et al., 1997, 1998b; Andersson et al., 1998; Czisch and Boelens, 1998; Meissner et al., 1998; Weigelt, 1998; Loria et al., 1999; Rance et al., 1999; Zhu et al., 1999) and the sensitive $^{1}H_N/^{15}N$ approach suggested by Yang and Kay (1999a, b) which does not actively suppress the anti-TROSY contribution. Here a simple modification is reported which results in the suppression of the anti-TROSY contribution, so that a more sensitive TROSY implementation becomes useable in 3D NOESY experiments.

Structural studies of large proteins rely substantially on the use of transverse relaxation-optimized methodologies that provide the necessary high spectral resolution and sensitivity through the constructive cancellation of interactions that otherwise contribute to rapid nuclear spin relaxation. In the case of the $^{1}H_N/^{15}N$ spin pair, the advantage arising from cross-correlation of dipole–dipole and chemical shift anisotropy mechanisms is greatest at the highest magnetic fields currently available and when used on samples with as complete a level of protein side chain deuteration as possible (Pervushin, 2000; Venters et al., 2002). Many TROSY adaptations to 3D and 4D triple-resonance experiments have been presented over the years, opening up the possibility for full structural studies of, and the mapping of molecular interactions in systems >100 kDa molecular weight (Salzmann et al., 1998, 2000; Yang and Kay, 1999a; Fernandez et al., 2001, 2004; Fiaux et al., 2002; Tugarinov et al., 2002; Oxenoid et al., 2004).

The basic concepts and mechanisms of transverse relaxation optimized spectroscopy have been reviewed in detail elsewhere (Pervushin, 2000). In brief, the TROSY approach combines several spectroscopic features that contribute to the superior linewidth, spectral resolution and sensitivity of such experiments. The most important of these features are: the use of the slowly relaxing multiplet component in an IS spin-system resulting from the constructive interference of dipole–dipole and chemical shift anisotropy interactions; the minimization of the periods where slow and fast relaxing spin-states are

*To whom correspondence should be addressed. E-mail: dn0@bio.cam.ac.uk

mixed; the complete single-transition to single-transition coherence transfer of $S_{x,y}I^{\beta}$ to $I_{x,y}S^{\beta}$ rather than to $I_{x,y}(S^{\alpha}+S^{\beta})$ resulting in a theoretical two-fold improvement of the transfer efficiency over a simple INEPT transfer step; the co-addition of I and S spin steady-state magnetization; the possibility of using both shift modulated orthogonal components, allowing the implementation of sensitivity enhanced echo/anti-echo detection without the need to extend the length of the pulse scheme; and finally, the simplification of the resulting spectrum, by selecting for the slowest relaxing component.

Results and discussion

Several versions of TROSY implementations have been published over the last few years; they can be grouped into two general categories. The first is ST2-PT (single-transition to single-transition polarization transfer) related experiments, introduced by Pervushin et al., which employ two sequential spin-state selective coherence transfer elements (S3CT) (Sorensen et al., 1997; Meissner et al., 1998); these experiments may use phase cycling or gradient P/N-type coherence selection (Pervushin et al., 1997, 1998b; Andersson et al., 1998; Czisch and Boelens, 1998; Meissner et al., 1998; Weigelt, 1998; Loria et al., 1999; Rance et al., 1999; Zhu et al., 1999). The second group consists of the enhanced gradient selection approach introduced by Yang and Kay (1999a, b).

In the first group of experiments the coherence transfer achieved during the back transfer from ^{15}N to ^{1}H before the detection period is equivalent to the effect of two subsequent spin-state selective 180° pulses to ^{15}N and ^{1}H transitions. This results in the correlation of the slowly relaxing ^{15}N multiplet component with the slowly relaxing proton multiplet component. The achieved spin-state selective transfer can be represented as

$$N_{\pm}(1-2H_z) \rightarrow H_{-}(1+2N_z), \qquad (1)$$

with the separate echo and anti-echo spectra only containing the TROSY line. During the back transfer magnetization proceeds via transverse and multiple quantum coherences that relax rapidly in large molecules.

In the second experimental scheme the back transfer from ^{15}N to ^{1}H employs a procedure reminiscent of the sensitivity enhanced pulsed field gradient sequence (Cavanagh et al., 1991; Kay et al., 1992; Schleucher et al., 1993). Again, both orthogonal shift modulated components are transferred, but as both coherence pathways are preserved this leads to the appearance of two diagonally shifted TROSY and anti- TROSY lines in the spectrum. The achieved coherence transfer is equivalent to the result produced by the action of an effective planar coupling Hamiltonian $H^{eff} = \pi J(2H_xN_x + 2H_yN_y)$ (Schulte-Herbruggen et al., 1991; Sattler et al., 1995a, b) and results in the transfer (Meissner et al., 1997).

$$N_{\pm}(1 \pm 2H_z) \rightarrow H_{-}(1 \mp 2N_z). \qquad (2)$$

While both experimental schemes provide the wanted TROSY line, the direct advantage of the planar coupling implementation comes from its inherently higher sensitivity as a consequence of slower relaxation during the coherence transfer steps. As shown by Yang and Kay, relaxation losses are minimized because for substantial amounts of time some of the operators leading to observable signal are stored as slowly relaxing terms along the z-axis (Yang and Kay, 1999b).

Further factors such as e.g. the choice of the water suppression scheme or additional coherence transfer steps in a pulse sequence can make a direct performance comparison of experiments based on the two TROSY schemes difficult. For example, triple-resonance experiments using a ST2-PT implementation allow a concatenation of the final ^{13}C to ^{15}N refocusing step with the first INEPT period of the ST2-PT module (Salzmann et al., 1999). Taking this into account, both triple-resonance TROSY implementations may give similar sensitivity.

Originally the second pulse scheme was introduced for amide proton detected TROSY-based triple-resonance experiments (Yang and Kay, 1999a, b). During the long constant-time periods in such experiments fast relaxation of the $N_{\pm}(1+2H_z)$ coherence results in strong attenuation of the pathway leading to the anti-TROSY signal. The ^{15}N transfer periods therefore act as transverse relaxation filters suppressing the unwanted lines and leaving the dominant features as those arising from the TROSY pathway.

However, this situation is in strong contrast to all experiments that lack this passive attenuation mechanism through the absence of such extended ^{15}N transfer periods. The lack of suppression of the anti-TROSY peaks will therefore lead to considerable spectral overlap, compromise the resolution and may cause confusion. Complete removal of the anti-TROSY line is thus crucial in such experiments. Similarly, the attenuation of the anti-TROSY lines will be incomplete in triple-resonance experiments performed on slowly relaxing systems, such as residues in flexible parts of a protein or smaller molecular weight systems. In such cases active anti-TROSY line suppression can be achieved through additional incorporation of a spin-state selective excitation (S3E) filter (Pervushin et al., 1998a; Yang and Kay, 1999a). Unfortunately S3E-suppression of the anti-TROSY line leads to a signal loss so that in the final analysis both categories of TROSY experiments have rather similar sensitivity.

In this contribution we show that a simple modification of the original Yang and Kay planar coupling TROSY approach (Yang and Kay, 1999b) results in the elimination of the anti-TROSY line without lengthening the sequence or introducing an additional spin-state selective filter. Thus the higher sensitivity of the planar coupling approach when compared to the ST2-PT scheme can therefore be achieved. Figure 1a displays the original pulse sequence and the alterations to the phases of the pulses which lead to the new sequence shown in Figure 1b. The new sequence is obtainable by a simple change of the phase of the last ^{1}H 90° pulse to y and the interchange of the pulse phases of the two last ^{15}N 90° pulses. To allow the control of the water resonance in the usual water-flip back fashion, a water-selective 90° pulse is introduced after the first ^{1}H 90° pulse of the back transfer scheme to assure the return of the water magnetization to $+z$ at the beginning of the acquisition (Grzesiek and Bax, 1993).

To understand the effect of these phase changes on the experimental outcome, the evolution of the relevant terms in both experiments is compared in Table 1. Terms Ia–IVa (Ib–IVb) represent the evolution in the experiments shown in Figures 1a, b. Apart from the trivial differences to the overall signal phase, it can be seen that the change of the 90° S pulse phase at point *c* from y to x leads to a different *J* evolution of the coherences originating from terms I and II. For Ia and IIa, one of the terms evolves under *J* during a first 2Δ period (b–c), while the other one is kept as MQ coherence. Subsequently, the other term evolves under *J* while the remaining one stays MQ during the second 2Δ period (d–e). This is typical of the situation where a sensitivity enhancement scheme is employed. In contrast to this, in the modified experiment only term Ib evolves under *J* but this time during both 2Δ periods, while term IIb remains MQ for all this time. As a net result of this modified evolution, *J* refocusing of the terms present at the end of t_1 becomes therefore not only dependent on the initial in-phase or anti-phase state but also on the orientation of the coherence along the x- or y-axis, while for terms Ia–IVa *J* refocusing depends solely on the initial in-phase or anti-phase character. With this, at point *f*, terms Ia–IVa in the Yang and Kay sequence are divided into two groups of observables with identical modulation in t_1 and t_2 i.e. the TROSY and anti-TROSY lines (Table 1). The sequence of Figure 1b on the other hand generates four observable terms with their individual t_1 and t_2 modulations that coadd to produce the single TROSY line.

Alternatively, the mixing scheme of the original implementation by Yang and Kay produces a heteronuclear ZQ/DQ π rotation that corresponds to $\pi(I_xS_x + I_yS_y)$ and leads to the transformation

$$I^{\alpha/\beta}S_- \rightarrow \pm iI_-S^{\alpha/\beta}. \quad (3)$$

Strictly speaking this transformation is preceded by a $(\pi/2)$ *z*-rotation to spins *I* and *S*. The phase changes suggested in Figure 1b transform the overall rotation into two subsequent bilinear rotations that are surrounded by two 90° rotations to either spin *I* or *S*; the resulting transformation is

$$\pi/2(S_y) - \pi(2I_xS_x + 2I_yS_y) - \pi/2(I_x) \quad (4)$$

This is identical to the overall rotation achieved by the two sequential S3 coherence transfer elements in the ST2-PT TROSY experiment, so that the transfer

$$I^{\beta}S_- \rightarrow \pm iI_-S^{\beta}, \quad (5)$$

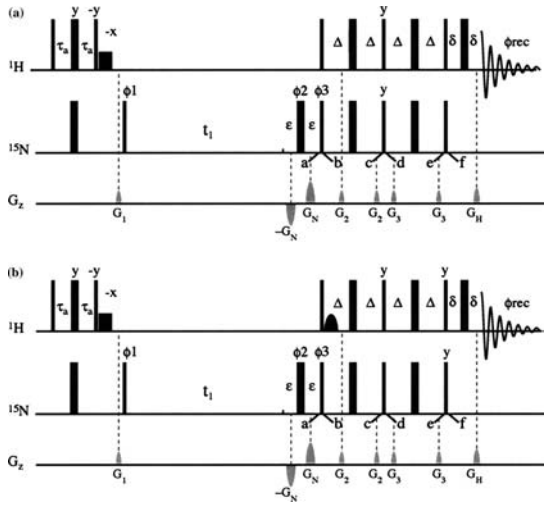

Figure 1. 2D [^{1}H, ^{15}N] TROSY pulse sequences based on the sensitivity enhanced planar coupling transfer pulse scheme. (a) Pulse sequence derived from the scheme previously implemented in triple-resonance experiments suggested by Yang and Kay (1999b). (b) Modified sequence proposed in this paper that results in the suppression of the anti-TROSY line. Narrow and wide bars correspond to 90° and 180° pulses, respectively; pulses are phase x unless otherwise indicated. A low-power 1.4 ms square 90° water flip-back pulse is represented by a small black rectangle, while a selective 90° E-SNOB (Kupce et al., 1995) water pulse of 2.1 ms is shown as shape. The pulse phases are $\phi_1 = (x, -x)$; $\phi_2 = (x, x, -x, -x)$; $\phi_3 = x$, with the receiver $\phi_{rec} = (x, -x)$. Quadrature detection and coherence pathway selection in the ^{15}N dimension are obtained using gradient selection (Kay et al., 1992; Schleucher et al., 1993). Echo/anti-echo pathways are recorded separately by inverting the amplitude of the split gradient G_N together with the inversion of ϕ_3. In addition, phase ϕ_1 and ϕ_{rec} are inverted with each t_1 increment (Marion et al., 1989). The magnitudes of G_1,G_2, G_3, G_N and G_H are 6.5, 5.0, 9.0, 30.5 and 10.3 G cm^{-1} with durations 1.5, 0.5, 0.5, 1.0 and 0.6, respectively. The delays τ_a, Δ, ε and δ are 2.3, 2.75, 1.0 and 0.65 ms, respectively.

is of the required outcome. Observation of the corresponding anti-echo is usually achieved by phase inversion of a 90° S pulse. A step-by-step analysis of the transfer pathways, and comparison with the scheme of Yang and Kay in Table 1 reveals, that in both experiments operators spend equal amounts of time either in the transverse plane or along the z-axis (Yang and Kay, 1999b). The effect of relaxation on both sequences is therefore very similar.

Figure 2 shows a region from the 2D [^{1}H, ^{15}N]- TROSY spectra of a 0.9 mM ^{15}N, ^{13}C, ^{2}H [Ile(δ_1 only), Leu, Val]-methyl-protonated sample of H-Ras (l-171)-GDP recorded at 4 °C with the two sequences depicted in Figure 1. The improved spectral resolution resulting from the suppression of the anti-TROSY line is evident. The correlation time of the protein under these conditions is 28 ns (Nietlispach et al., 2002). A comparison of the intensities of 50 randomly selected TROSY lines in these spectra, and also in 2D ^{1}H/^{15}N planes of a TROSY-HNCO experiment recorded at 800 MHz, revealed that to within the experimental error, both versions of the pulse sequences shown in Figure 1 give spectra with identical sensitivity. The level of anti-TROSY line suppression in the new scheme is comparable to the ST2-PT sequence.

Under similar experimental conditions, a comparison of 3D TROSY-HNCA spectra showed that the modified sequence is on average 8–10% (at a correlation time of 11 ns) and 15% (at 28 ns) more sensitive than a sequence using an ST2-PT back transfer pulse scheme with concate-

Table 1. Evolution of observable terms in pulse sequences of Figure 1[A]

Term[B]	a	b	c	d	e	f	t_2[C]	t_1[D]
Ia	S_x	S_x	$2S_yI_z$	$2S_yI_x$	$-2S_yI_x$	$-2S_zI_x$	$-2I_-S_z$	$(e^+ - e^-)$
IIa	$2S_xI_z$	$-2S_xI_y$	$2S_xI_y$	$-2S_zI_y$	I_x	I_x	I_-	$(e^+ + e^-)$
IIIa	$2S_y$	S_z	$-S_z$	$-S_x$	$-2S_yI_z$	$2S_zI_y$	$-2I_-S_z$	$(e^+ - e^-)$
IVa	$2S_yI_z$	$-2S_zI_y$	I_x	$-I_z$	I_z	$-I_y$	I_-	$(e^+ + e^-)$
Ib	S_x	S_x	$2S_yI_z$	$2S_zI_x$	$-I_y$	$-I_y$	$-iI_-$	$(e^+ - e^-)$
IIb	$2S_xI_z$	$-2S_xI_y$	$2S_xI_y$	$2S_xI_y$	$-2S_xI_y$	$2S_zI_y$	$I2I_-S_z$	$(e^+ + e^-)$
IIIb	$2S_y$	S_z	$-S_z$	S_y	$2S_xI_z$	$-2S_zI_x$	$I2I_-S_z$	$(e^+ - e^-)$
IVb	$2S_yI_z$	$-2S_zI_y$	I_x	$-I_z$	I_z	I_x	$-iI_-$	$(e^+ + e^-)$

[A]Positions of time points a–f are indicated in the pulse sequences of Figure 1. [B]Terms Ia–IVa and Ib–IVb correspond to the evolution of observable terms in Figures 1a and b, respectively. Only the evolution of S_+ coherence, with ϕ_3 set to x is shown. For simplicity it is assumed that γ_I, γ_s and $^1J_{I,S}$ are positive. [C]Co-addition of terms Ia–IVa results in $I_-(1-2S_z)e^+ + I_-(1+2S_z)e^-$ while the sum of Ib–IVb gives $-iI_-(1-2S_z)e^+$. [D]e^+ and e^- describe the t_1 evolution of the two multiplet components $e^{-i(\Omega+\pi)}$ and $e^{-i(\Omega-\pi)}$, respectively.

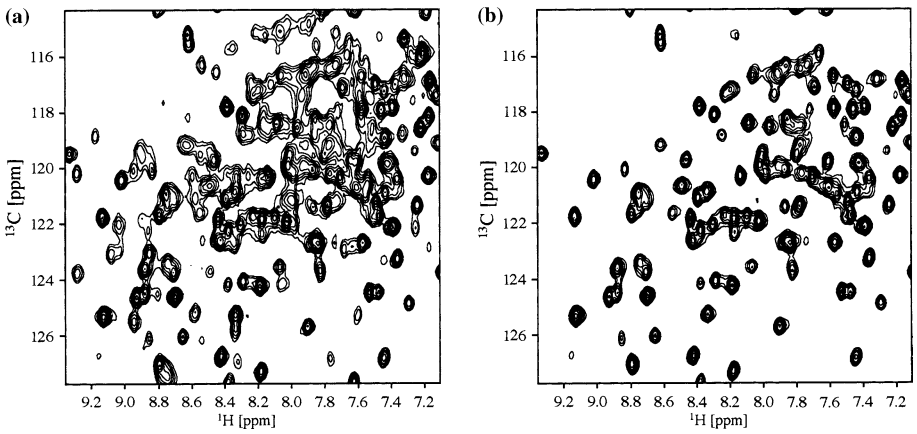

Figure 2. Part of the 2D [^{1}H, ^{15}N] TROSY spectra acquired with the two pulse schemes shown in Figure 1. (a) The non-suppressed experiment and (b) the anti-TROSY line suppressed spectrum (pulse sequence Figure 1b) recorded at 4 °C ($\tau_c \sim 28$ ns) on a 0.9 mM ^{15}N, ^{13}C, ^{2}H [Ile(δ_1 only), Leu, Val]-methyl-protonated sample of H- Ras (1-171)-GDP. All spectra were recorded on a Bruker DRX 800 spectrometer.

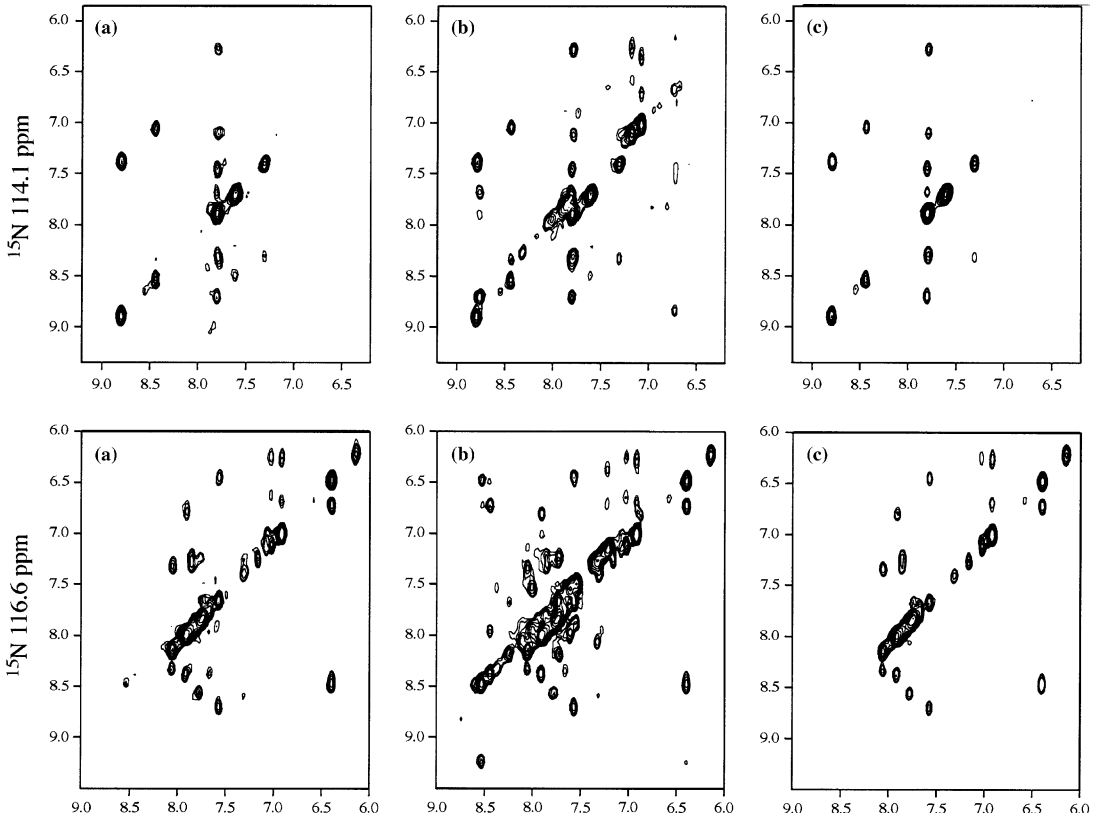

Figure 3. 2D cross-sections taken from ^{15}N separated NOESY TROSY spectra (at ^{15}N = 114.1, 116.6 ppm) ($\tau_m = 100$ ms) recorded using (a) the modified implementation of Figure 1b, (b) the non-suppressed version shown in Figure 1a and (c) a ST2-PT TROSY implementation (Zhu et al., 1999), respectively. Spectra were recorded with 32 (^{15}N) × 90 (^{1}H) FIDs, each with 8 scans. Spectral widths in the three dimensions were (2000 Hz) (^{15}N), 8800 Hz (^{1}H) and 10000 Hz (^{1}H).

nated ^{13}C, ^{15}N refocusing. These results are in close agreement with the observations reported by Yang and Kay (1999a). As the modified sequence leads to no additional loss in sensitivity it can be used in the triple-resonance experiments instead of the original scheme, thus guaranteeing the suppression of anti-TROSY lines of very flexible residues; there is no need to introduce an additional S3E filter.

The main benefit of the new scheme is evident in ^{15}N separated NOESY type experiments, where the higher transfer efficiency due to the planar coupling scheme is particularly attractive but only useful when combined with the complete suppression of the anti-TROSY line; this is provided by the new sequence. Figures 3a and c show 2D $^{1}H/^{1}H$ planes of 3D NOESY-[^{1}H, ^{15}N]-TROSY experiments where the slightly improved performance of the modified scheme is evident when compared with an ST2-PT implementation of the same experiment. Similar sensitivity improvements as mentioned above for the triple-resonance experiments are observed in the 3D NOESY spectrum using the new scheme. Figure 3b shows the same planes without anti-TROSY line suppression using the implementation of Figure 1a. The extensive crowding underlines the necessity for efficient anti-TROSY line suppression.

Conclusions

In conclusion, a simple pulse sequence modification is introduced that suppresses the anti-TROSY line contribution in experiments using the planar coupling style TROSY transfer implementation previously suggested for constant-time triple-resonance experiments. In the new experiment, suppression is achieved without a sensitivity penalty, as a result, the higher sensitivity transfer scheme becomes useable in 3D/4D ^{15}N separated NOESY-TROSY experiments. Alternatively it can be used to remove the anti-TROSY line in triple-resonance experiments.

Acknowledgements

The NMR facility of the Department of Biochemistry is supported by BBSRC and the Welcome Trust. Drs Yutaka Ito and Minoru Hatanaka are thanked for the kind donation of the H-Ras sample. Dr James Keeler is thanked for stimulating discussions.

References

Andersson, P. et al. (1998) *J. Magn. Reson.*, **133,** 364–367.
Cavanagh, J. et al. (1991) *J. Magn.* Reson., **91**, 429–436.
Czisch, M. and Boelens, R. (1998) *J. Magn. Reson.,* **134,** 158–160.
Fernandez, C. et al. (2001) *Proc. Natl. Acad Sci. USA,* **98**, 2358–2363.
Fernandez, C. et al. (2004) *J. Mol. Biol.,* **336**, 1211–1221.
Fiaux, J. et al. (2002) *Nature*, **418,** 207–211.
Grzesiek, S. and Bax, A. (1993) *J. Am. Chem. Soc.,* **115,** 12593–12594.
Kay, L.E. et al. (1992) *J. Am. Chem. Soc.,* **114,** 10663–10665.
Kupce, E. et al. (1995) *J. Magn. Reson. Ser. B,* **106**, 300–303.
Loria, J.P. et al. (1999) *J. Magn. Reson.,* **141**, 180–184.
Marion, D. et al. (1989) *J. Magn. Reson.,* **85**, 393–399.
Meissner, A. (1997) *J. Biomol. NMR*, **10**, 89–94.
Meissner, A. et al. (1998) *Mol. Phys.*, **95,** 1137–1142.
Nietlispach, D. et al. (2002) *J. Am. Chem. Soc.,* **124,** 11199–11207.
Oxenoid, K. et al. (2004) *J Am. Chem. Soc.*, **126,** 5048–5049.
Pervushin, K. (2000) *Q. Rev. Biophys.,* **33,** 161–197.
Pervushin, K. et al. (1997) *Proc. Natl. Acad. Sci. USA,* **94,** 12366–12371.
Pervushin, K. et al. (1998a) *J. Am. Chem. Soc.,* **120**, 6394–6400.
Pervushin, K. et al. (1998b) *J. Biomol. NMR,* **12,** 345–348.
Rance, M. et al. (1999) *J. Magn. Reson.,* **136**, 92–101.
Salzmann, M. et al. (1998) *Proc. Natl. Acad. Sci. USA*, **95,** 13585–13590.
Salzmann, M. et al. (2000) *J. Am. Chem. Soc.,* **122**, 7543–7548.
Salzmann, M. et al. (1999) *J Biomol. NMR,* **15,** 181–184.
Sattler, M. et al. (1995a) *J. Magn. Reson. Ser. B,* **108**, 235–242.
Sattler, M. et al. (1995b) *J. Biomol. NMR,* **6**, 11–22.
Schleucher, J. et al. (1993) *Angew. Chem.-Int. Edit. Engl.*, **32**, 1489–1491.
Schulte-Herbruggen, T. et al. (1991) *Mol. Phys.,* **72,** 847–871.
Sorensen, M.D. et al. (1997) *J. Biomol. NMR,* **10,** 181–186.
Tugarinov, V. et al. (2002) *J. Am. Chem. Soc.,* **124,** 10025–10035.
Venters, RA. et al. (2002) *J. Mol. Struct.,* **602,** 275–292.
Weigelt, J. et al. (1998) *J. Am. Chem. Soc.,* **120,** 10778–10779.
Yang, D.W. and Kay, L.E. (1999a) *J. Am. Chem. Soc.,* **121,** 2571–2575.
Yang, D.W. and Kay, L.E. (1999b) *J. Biomol. NMR,* **13,** 3–10.
Zhu, G. (1999) *J. Biomol. NMR,* **13,** 77–81.